

Structure of carbohydrate-bound polynuclear iron oxyhydroxide nanoparticles in parenteral formulations

Dina S. Kudasheva^{a,b}, Jriuan Lai^{a,b,c}, Abraham Ulman^{a,b,c}, Mary K. Cowman^{a,b,*}

^a Othmer Department of Chemical and Biological Sciences and Engineering, Polytechnic University, Six Metrotech Center, Brooklyn, NY 11201, USA

^b Herman F. Mark Polymer Research Institute, Polytechnic University, Six Metrotech Center, Brooklyn, NY 11201, USA

^c The NSF MRSEC for Polymers at Engineered Interfaces, Polytechnic University, Six Metrotech Center, Brooklyn, NY 11201, USA

Received 21 January 2004; received in revised form 28 April 2004; accepted 11 June 2004

Available online 11 September 2004

Abstract

Intravenous iron therapy is used to treat anemia associated with chronic kidney disease. The chemical structures of parenteral iron agents have not been characterized in detail, and correlations between structure, efficiency of iron delivery, and toxicity via catalysis of oxygen-derived free radical creation remain to be established. In this study, two formulations of parenteral iron have been characterized by absorption spectroscopy, X-ray diffraction analysis (XRD), transmission electron microscopy (TEM), atomic force microscopy (AFM), and elemental analysis. The samples studied were Venofer[®] (Iron Sucrose Injection, USP) and Ferrlecit[®] (Sodium Ferric Gluconate in Sucrose Injection). The 250–800-nm absorption spectra and the XRD patterns showed that both formulations contain a mineral core composed of iron oxyhydroxide in the β -FeOOH mineral polymorph known as akaganeite. This was further confirmed for each formulation by imaging using TEM and AFM. The average core size for the nanoparticles, after dialysis to remove unbound or loosely bound carbohydrate, was approximately 3 ± 2 nm for the iron–sucrose, and approximately 2 ± 1 nm for the iron–gluconate. Each of the nanoparticles consists of a mineral core, surrounded by a layer of bound carbohydrate. The overall diameter of the average bead in the dialyzed preparations was approximately 7 ± 4 nm for the iron–sucrose, and 3 ± 1 nm for the iron–gluconate. Undialyzed preparations have particles with larger average sizes, depending on the extent of dilution of unbound and loosely bound carbohydrate. At a dilution corresponding to a final Fe concentration of 5 mg/mL, the average particle diameter in the iron–sucrose formulation was approximately 22 ± 9 nm, whereas that of the iron–gluconate formulation was approximately 12 ± 5 nm.

© 2004 Elsevier Inc. All rights reserved.

Keywords: Parenteral formulations; Iron oxyhydroxide; Iron–carbohydrate complex; AFM; Iron–sucrose injection; Sodium ferric gluconate; Akaganeite

1. Introduction

Parenteral iron formulations containing iron complexed to monosaccharides or disaccharides are among the products currently used for the treatment of anemia.

Yet, the chemical structures of these materials have not been characterized in detail, and correlations between structure and complex stability, efficiency of iron delivery, and toxicity via catalysis of oxygen-derived free radical creation remain to be established. This study represents a first step toward complete characterization of the structures of this subclass of modern therapeutic iron–carbohydrate compounds.

Iron(III) oxyhydroxide is formed in aqueous solutions by the dissolution of a suitable iron salt, such as ferric chloride, at low pH, followed by neutralization

* Corresponding author. Tel.: +1 718 260 3054; fax: +1 718 260 3125.

E-mail address: mcowman@poly.edu (M.K. Cowman).

or basification [1–3]. The aquated iron ions are hydrolyzed initially to the mononuclear iron hydroxides $\text{Fe}(\text{OH})(\text{H}_2\text{O})_5$ and $\text{Fe}(\text{OH})_2(\text{H}_2\text{O})_4$. Formation of $\text{Fe}(\text{OH})_3(\text{H}_2\text{O})_3$ leads to the growth of a polynuclear (containing multiple linked iron atoms) iron oxyhydroxide with the approximate composition FeOOH . This mineral is insoluble unless stabilized by the presence of a water-soluble chelating agent.

Carbohydrates can be appropriate chelating agents for the stabilization of iron oxyhydroxide nanoparticles in colloidal suspension. Certain low molecular mass neutral carbohydrates, such as sucrose [4], or fructose [5] present multiple hydroxyl groups in a suitable array to chelate iron, although the binding is inherently weak in neutral aqueous solution. Polymeric carbohydrates such as dextran may also be used to stabilize nanoparticles because they present a large number of hydroxyl groups, which can cooperatively chelate the surface of iron oxyhydroxide nanoparticles. For a neutral carbohydrate, the chelation to iron is enhanced at high pH, because the hydroxyl groups may become deprotonated, thus acquiring a negative charge, and interacting more strongly with the cationic iron ion [6]. At neutral pH, inherently anionic carbohydrates such as gluconate or partially oxidized polysaccharides are more effective nanoparticle stabilizers. In these cases, a carboxyl group provides the negative charge over a broad pH range. Its chelation to iron can also drive the deprotonation of nearby hydroxyl groups, further enhancing the complex stability [4,7].

The structures of complexes formed between iron nanoparticles and polysaccharides have been studied previously, because iron–dextran complexes [8,9] and iron–polymaltosate complexes [10–12] (where polymaltosate was the commercial name for partially hydrolysed and oxidized starch) have been used for decades in the treatment of anemia. In a number of cases, the nanoparticle cores have been identified as iron oxyhydroxide. X-ray diffraction data are most consistent with the akaganeite ($\beta\text{-FeOOH}$) polymorph (polymorphs are solids with the same chemical composition but different crystal structures) [13–18]. Ultra-violet–visible (UV–VIS) absorption spectroscopy [5,17–19] and Mössbauer spectroscopy [13–16,20] have shown the presence of octahedrally coordinated high-spin Fe(III) ions. Extended X-ray absorption fine structure (EXAFS) studies [14] confirm the coordination of iron by 6 oxygen atoms, at an Fe–O distance of 1.95 Å, and the location of a somewhat disordered shell of iron ions at a distance of about 3.05 Å. The iron oxyhydroxide crystallite dimensions estimated from the broadening of X-ray diffraction peaks are generally about 1–5 nm in diameter [9,14,17]. Electron microscopy has shown that the dimensions of the core (which may be larger than the size of the crystalline portion) can range from 3 nm diameter spheres [9] to ellipsoidal particles with dimensions of up to

5×34 nm [21]. The mineral core is stabilized by interactions with the polysaccharide, presumably through the hydroxyl and/or carboxyl groups of the carbohydrate units, the latter having been generated by partial oxidation of the polysaccharide. The overall particle size is highly dependent on the nature of the polysaccharide and the mode of complex formation. An older commercial iron–dextran complex had a reported overall diameter of about 12–13 nm [9], whereas iron complexes with κ -carrageenan are reported to form 25–50 nm aggregates of 10–20 nm particles [17,18]. The apparent complex molecular mass, based on elution position in gel permeation chromatography (GPC) chromatograms, may range from 72 kDa (InFed[®]) to 90 kDa (Imferon[®]) to 265 kDa (Dexferrum[®]).

Information about the structure of iron complexes with low molecular mass carbohydrates has been predominantly derived from studies of soluble mono- or di-nuclear iron complexes. Weakly stable mononuclear complexes are formed by carbohydrates with structures that allow at least three hydroxyl groups to interact simultaneously with a single iron ion. For example, sucrose or its component sugar fructose can bind iron weakly at neutral pH [4–6]. There is much less information about complexes containing polynuclear iron species complexed with monosaccharides or disaccharides. Studies of ferric fructose systems suggested that the fructose may serve primarily to coat iron-containing particles at neutral pH. Interestingly, when the pH is raised, the formation of a tetra-deprotonated sugar moiety was proposed to break down the polynuclear iron to the mononuclear ferric fructose complexes. It was also noted that gluconate, with its carboxyl group, was much more effective in breaking down the particles [5]. For iron sucrose, earlier studies suggest the presence of polynuclear iron complexed with sucrose, in which the mineral core has been proposed to be a 2-line ferrihydrite [22] rather than an iron oxyhydroxide.

Some of the questions that may arise in the analysis of polynuclear iron–carbohydrate complexes include: (1) the composition and polymorphic form and degree of crystallinity of the iron mineral component, (2) the size and shape of the nanoparticles, (3) the stability of the nanoparticles, (4) the location of the saccharide component within the particle, (5) the molar ratio of iron to saccharide, and (6) the mode of binding between the iron and saccharide components, including the extent of saccharide deprotonation in the complex. In the present work, we address some of these questions by examining two different iron–carbohydrate complexes with respect to the mineral environment of the iron, the nanoparticle size, and the particle stability upon dilution or separation from unbound carbohydrate by dialysis.

2. Materials and methods

The parenteral iron formulations used in this study were an iron–sucrose (Venofer[®], Iron Sucrose Injection, USP, lots 1644 and 2323A), from American Regent, Inc., Shirley, NY, and an iron–gluconate in sucrose (Ferrlecit[®], Sodium Ferric Gluconate Complex in Sucrose Injection, lots 1F541 and 1C239), from Watson Pharmaceuticals, Inc., Corona, CA. Venofer[®] was supplied as the iron–sucrose complex in 5 mL vials containing 100 mg of elemental iron in 30% sucrose solution (20 mg Fe/mL) at a pH of about 10.5–11.1. The apparent average molecular mass is stated in the package insert to be 34–60 kDa. Ferrlecit[®] was obtained as the iron–gluconate complex in 5 mL ampules containing 62.5 mg of elemental iron as a sodium salt of a ferric gluconate complex in 20% sucrose (12.5 mg Fe/mL) at a pH of about 7.7–9.7. The apparent average molecular mass is stated in the package insert to be 350 ± 23 kDa. Some samples, where noted in the text, were subjected to dialysis to remove low molecular mass components. Dialysis of samples for absorption spectroscopy was performed against deionized water, at a pH of about 5.4, in Slide-A-Lyzer Dialysis Cassettes (Pierce, Rockford, IL) made of low-binding regenerated cellulose membrane, molecular weight cutoff (MWCO) 10,000. Cassette capacity was 0.5–3 mL. Larger volumes of dialyzed samples were needed for AFM and TEM studies; in that case dialysis against deionized water at neutral pH, or with pH adjusted with KOH to match the sample pH, was performed in tubes made of Spectra/Por Molecularporous Regenerated Cellulose Membrane (Spectrum Laboratories Inc., Rancho Domingues, CA) with MWCO 6–8,000. Dialysis time for both trials was 20–48 h. Dialyzed samples were sent to Huffman Laboratories, Inc. (Golden, CO) for elemental analysis to determine the amount of iron, carbon and sodium.

Absorption spectra were recorded on a Perkin–Elmer Lambda 800 UV/VIS absorption spectrophotometer. The spectra were analyzed with UV WinLab software v3.00.03. The spectra were recorded in the range of 800–200 nm for original non-diluted samples and for diluted or dialyzed samples. This instrument has the ability to analyze samples with relatively high absorbance. Its photometric linearity at an absorbance (A) of 3 is ± 0.006 A units and at A of 2 is ± 0.002 A units. The photometric accuracy at A of 2 is ± 0.003 A units and stray light in the range of 220–370 nm is <0.00008% T. The photometric range is ± 7 A. For the undiluted samples, cylindrical quartz cells of path length 0.001 or 0.01 cm were employed; for all other samples a cylindrical quartz cell of path length 0.01 cm was used. The reference was water. All spectra were recorded as absorbance vs. wavelength of light in nm. Molar extinction coefficients were calculated from the absorbances at wavelengths of 300 and 470 nm, based

on the molar concentration of iron in each sample. The molar iron concentrations were calculated from the stated weight concentration of iron in each sample.

X-ray powder diffraction (XRD) patterns were recorded at a scanning rate of 0.008° min⁻¹ in the range 2θ from 0° to 70° using a Philips X-ray diffractometer with Cu Kα radiation (λ = 1.5418 Å). Original and dialyzed samples were prepared by freeze-drying prior to analysis. The average iron mineral crystallite size, *D*, was calculated from the observed XRD profiles using the peak full width at half maximum height (β) of the selected diffraction peak, using the Scherrer formula [23]:

$$D = K\lambda/\beta \cos \theta,$$

where *K* is the Scherrer constant, with a value of 0.94. For recorded crystalline patterns, diffraction angles and interplanar spacings obtained were compared with the values compiled in the JCPDS-ICDD (Joint Committee on Powder Diffraction Standard-International Center for Diffraction Data-copyright PSI International) reference cards.

Electron microscopic studies of the iron-core crystal size and morphology for the iron–carbohydrate samples were carried out by using a Phillips CM-12 Transmission Electron Microscope (100 keV). All preparations were deposited one night before imaging onto a carbon stabilized Formvar-coated copper grid (400 mesh), purchased from Ted Pella, Inc., Redding, CA. Approximate grid hole size is 42 μm, and the thickness of Formvar films stabilized with carbon is 5–10 nm. All attempts to image the original undiluted liquids were not successful, because the resulting film on a grid was too thick for electrons to penetrate. Consequently, the iron–carbohydrate complexes were dialyzed and the grid was dipped into the sample and then the excess liquid was removed with a very gentle flow of compressed nitrogen.

Atomic force microscopy (AFM) was used to determine size and shape of iron–carbohydrate complexes. The instrument used was a MultiMode Scanning Probe Microscope with Nanoscope IIIa controller and a type EV scanner (Veeco Instruments, Inc). The scanner was calibrated in the *x–y* plane using the 1 μm etched grid, and in the *z*-direction using the 200 nm height calibration standard. The samples for imaging were prepared in two ways. In the first procedure, samples were diluted 2 to 80-fold with deionized water prior to analysis. In the second procedure, samples were dialyzed against deionized water prior to analysis. In both cases, 4 μL of sample was put on a freshly cleaved mica surface, then after 20–30 s the surface was rinsed with 100 μL of deionized water to get rid of unbound particles, and the surface was dried by a gentle flow of nitrogen. The AFM imaging technique used was Tapping ModeTM. TESP etched silicon cantilever probes of 125 μm nominal length were used, at a drive frequency of approximately 240–280 kHz. We generally use an RMS (root

mean square) voltage of approximately 2.5–3 V, and adjust the setpoint for optimum image, which is generally about 1 V below the RMS voltage. Both height and amplitude information were recorded at a scan rate of 2–3 Hz, and stored in a 256 × 256 pixel format. Images were processed using the Nanoscope version 4.43r8 software. For optimum clarity in visual presentation of the nanoparticle images in the figures, flattening of first order was employed unless stated otherwise. For images to be used in measuring heights, the only image processing was zero order flattening. These images were analyzed to determine height and diameter of the particles observed. Although the height measurement is considered accurate, the apparent particle diameter is broadened by the finite dimensions of the probe tip. A correction for the tip broadening effect has been made following the procedure of Margeat et al. [24]. The apparent diameter measured at half height, S , is related to the real diameter, D , and the tip radius, R , according to the following equation [24]:

$$S = 2 \left(RD + \frac{D^2}{4} \right)^{1/2}.$$

The tip radius was estimated by imaging DNA, which has a real chain diameter of 2 nm. For one AFM tip used, the measured apparent diameter of DNA at half height was 11.8 nm, resulting in an estimated tip radius of 16.8 nm. A second tip had an estimated radius of 14.8 nm. The appropriate tip radius was used to estimate corrected diameters in our images, although we may expect some minor variation for a given tip as a function of use. Thus the estimated particle diameters are subject to uncertainty on this basis. The relative diameters for a given series of samples differing in dilution were measured

on the same day and with a single tip, and should be representative of the effect of dilution on the particle diameter. The relative sizes of particles in different iron formulations were confirmed by analysis of all samples on the same day, using a single tip, and running a calibration image of DNA on the same occasion.

3. Results and discussion

3.1. Absorption spectroscopy

For Fe(III) in a high spin state octahedrally coordinated to oxygen, several characteristic absorption bands are expected. At 250–390 nm, a band of high intensity arises from oxo-metal charge transfer transitions, as has been reported for Fe(III)–glucose at 320 nm and for Fe(III)–sucrose at 370 nm [19]. Low intensity bands at 470–500 nm and 560–580 nm arise from d to d transitions of octahedral d^5 complexes of Fe(III). For low spin Fe(III), the latter bands would be of high intensity. The presence of Fe(II) would result in a band at 420–450 nm for the d–d transition of octahedral d^6 Fe(II), and a high intensity band at 800–900 nm for an aquated-Fe(II) complex [25].

The spectral shapes of the studied parenteral iron formulations show a weak absorption band at about 470–500 nm and a strong band about 300 nm. Fig. 1 shows the absorption spectra for the two samples after dilution to the same nominal concentration of 5 mg Fe/mL, to facilitate spectral shape comparison. The 470–500 nm band is attributed to the d–d transition of octahedral high spin d^5 Fe(III). The 300 nm band shows that the iron is chelated to oxygen, and is due to the oxo-metal

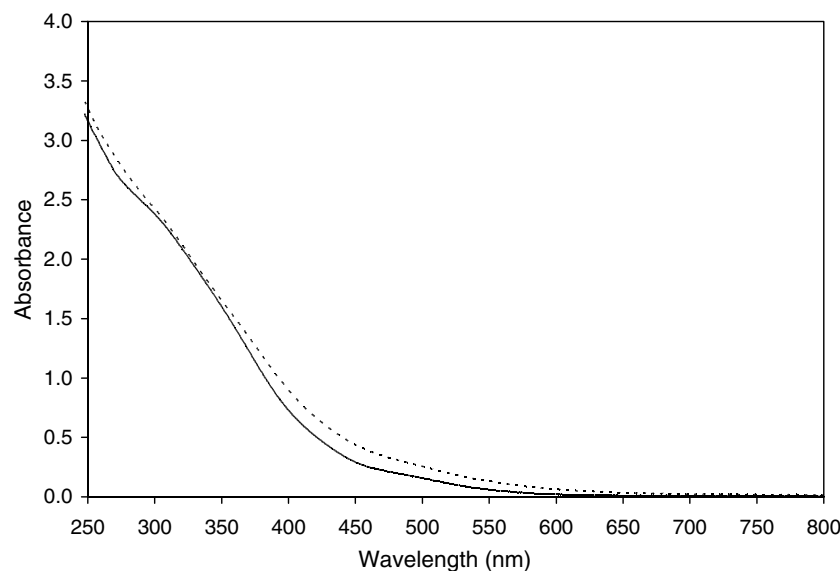


Fig. 1. Absorption spectra of iron–sucrose (dashed line), and iron–gluconate (solid line) diluted to nominal iron concentrations of 5 mg/mL and analyzed in an optical cell of 0.01 cm path length.

Table 1
Characterization of iron–carbohydrate complexes by absorption spectroscopy

Sample	Fe Conc. (mg/mL)	Cell path length (cm)	ϵ_{300} ($M^{-1} \text{ cm}^{-1}$)	ϵ_{470} ($M^{-1} \text{ cm}^{-1}$)	$\epsilon_{300}/\epsilon_{470}$
Iron–sucrose	20	0.001	2990		7.9
	20	0.01		380	
	5	0.01	2720	390	7.0
Iron–gluconate	12.5	0.001	2600		9.0
	12.5	0.01		290	
	5	0.01	2670	250	10.6

charge transfer absorption band. There is no evidence for the existence of low spin state Fe(III) or for aquated Fe(II). The shapes of the spectra are essentially the same for both iron–carbohydrate samples; both formulations showed characteristic absorption spectra expected for Fe(III) complexes in an octahedral d^5 high spin state.

The position of the $d-d$ transition band around 500 nm has been shown to depend on the distance between two neighboring Fe atoms [26]. Thus, in the case of face-sharing octahedra of an iron oxide hematite, this band is above 500 nm. For the edge- and corner-sharing octahedra and hence larger Fe–Fe distances in iron oxyhydroxides this transition is weaker and lies at shorter wavelengths of 470–499 nm [27]. Based on the fact that both iron formulations have this band at approximately the same position, we can conclude that the nature of the iron core is the same and both spectra are compatible with the expected ferric oxyhydroxide mineral form.

The molar extinction coefficients of the absorption bands for each sample were closely similar (Table 1). The peak at 300 nm was best quantitated in undiluted samples analyzed in an optical cell with a path length of 0.001 cm. Calculated extinction coefficients at 300 nm were approximately 2600–3000 $M^{-1} \text{ cm}^{-1}$ for the two samples. This compares with reported values of 6660 for a different iron–sucrose preparation [19] and 1700 for iron–carrageenan [17]. The shoulder at 470–

500 nm was best quantitated in undiluted sample analyzed in an optical cell with a 0.01 cm path length. The extinction coefficient at 470 nm was approximately 300–400 $M^{-1} \text{ cm}^{-1}$ for the two samples.

The stability of the iron core structure in each of the iron formulations was assessed by dilution and/or dialysis. Dilution to a concentration of 5 mg Fe/mL, or dialysis against water resulting in a similar dilution, had no significant effect on the spectral shape or molar extinction coefficients of the iron absorption bands (Table 1).

3.2. Transmission electron microscopy (TEM)

TEM micrographs of dialyzed iron–sucrose and dialyzed iron–gluconate samples at equivalent magnifications are compared in Fig. 2. The beadlike iron mineral cores appear to be fairly uniform in size for a given sample. This uniformity reflects the manufacturing processes, and results in particles with a narrow range of sizes. The comparison of the images of two samples shows that the iron–gluconate particles have cores that are generally slightly smaller (Fig. 2(a)) than those of iron–sucrose (Fig. 2(b)).

Measurement of the diameters of the electron dense particles is used to estimate the diameter of the iron mineral core in a given sample. For iron–sucrose, the results indicate a mineral core size distribution ranging from

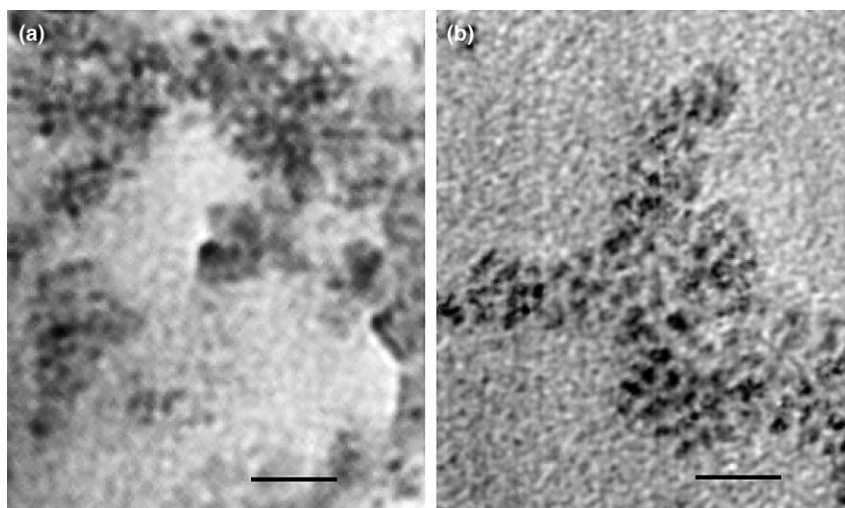


Fig. 2. Transmission electron microscopy image of (a) dialyzed iron–gluconate complex and (b) dialyzed iron–sucrose complex. The bar is 20 nm.

Explore Litigation Insights

Docket Alarm provides insights to develop a more informed litigation strategy and the peace of mind of knowing you're on top of things.

Real-Time Litigation Alerts



Keep your litigation team up-to-date with **real-time alerts** and advanced team management tools built for the enterprise, all while greatly reducing PACER spend.

Our comprehensive service means we can handle Federal, State, and Administrative courts across the country.

Advanced Docket Research



With over 230 million records, Docket Alarm's cloud-native docket research platform finds what other services can't. Coverage includes Federal, State, plus PTAB, TTAB, ITC and NLRB decisions, all in one place.

Identify arguments that have been successful in the past with full text, pinpoint searching. Link to case law cited within any court document via Fastcase.

Analytics At Your Fingertips



Learn what happened the last time a particular judge, opposing counsel or company faced cases similar to yours.

Advanced out-of-the-box PTAB and TTAB analytics are always at your fingertips.

API

Docket Alarm offers a powerful API (application programming interface) to developers that want to integrate case filings into their apps.

LAW FIRMS

Build custom dashboards for your attorneys and clients with live data direct from the court.

Automate many repetitive legal tasks like conflict checks, document management, and marketing.

FINANCIAL INSTITUTIONS

Litigation and bankruptcy checks for companies and debtors.

E-DISCOVERY AND LEGAL VENDORS

Sync your system to PACER to automate legal marketing.